SUPPLEMENTAL FIGURES 1-5

Activation of aortic endothelial cells by oxidized phospholipids: a phosphoproteomic analysis

Alejandro Zimman, Sharon S. Chen, Evangelia Komisopoulou, Bjoern Titz, Roxana Martínez-Pinna, Aarya Kafi, Judith A. Berliner, and Thomas G. Graeber.

Supplemental Figure 1. Mass spectrometry alignment and quantitation analysis pipeline. (a) Schematic of the quantitation procedure. The analysis pipeline first applies a time-warping algorithm published by Prakash et al. (reference 23). Several related versions and applications of chromatography alignment algorithms have also been published (references 24-28). The alignment algorithm works in two phases. First, it creates signal maps based on the raw MS time, mass to charge (m/z), and intensity data from each sample. Second, the algorithm detects common features (ion peaks) from these signal maps thus enabling their alignment. This information is combined with the identification of phosphopeptides via SEQUEST to localize and calculate maximal peak intensity across all samples. Step 1) The chromatography elution profiles (m/z vs time plots) of all samples are time-axis pairwise aligned using a time warping algorithm to find the optimal time alignment of the peaks. Step 2) Peptide peaks are sequence identified using MS2 collision spectra. Step 3) Peptide peaks sequenced in some samples but not others are located in the remaining samples via the chromatography profile alignment mappings. Step 4) Maximal peak intensity is then determined. Step 5) All peaks are visually inspected and manually corrected if necessary to ensure data quality.

To demonstrate the performance of the algorithm, we present data showing the alignment of the mass spectrometry profiles of the phospho-tyrosine peptide enriched samples. (b) Pre-alignment comparison of the elution times of phosphopeptides identified by fragmentation sequencing in both of a pair of samples. To provide a reference, all sample pairings graphed include the same x-axis sample (Experiment #2/Ox-treated/Run #2). The chromatography runs had similar elution profiles, except for one which was shifted by an approximately constant amount throughout the run, i.e. the elution gradient start time was delayed (Experiment #1/Control/Run #2, maroon circles). (c) Chromatography alignment of two sample runs by extracting common features (over 1,800 data points) from their signal maps and aligning these features by the time-warping dynamic programming algorithm (blue line). As a reference and positive control we overlay the elution times of peaks that were identified as the same phosphopeptide by fragmentation sequencing independently in both samples (open circles). (d) Post-alignment comparison of the elution times of phosphopeptides identified by fragmentation sequencing in both of a pair of samples.

(e) The chromatography elution profile of a representative phosphopeptide indicating the typical peak width in the time dimension. (f) Histogram showing the distribution of differences in elution times for the phosphopeptides sequenced in both of a pair of samples using the alignment corrected elution times of panel d. Following alignment, the vast majority of phosphopeptides had a difference in elution time of less than 30 seconds, which is smaller than the typical peak width of panel e. In other words, after alignment, the phosphopeptide peaks shared by both samples overlay each other in the elution time dimension.

The alignment algorithm does not use any of the sequencing information. Thus, these plots demonstrate the performance of the algorithm in aligning peaks between samples using the co-sequenced peaks as a control case. In the same fashion, the alignment results are then used to align cases where a phosphopeptide peak was sequenced in one sample but not in another. This allows the alignment-based identification of phosphopeptide peaks even in samples where they were not identified by fragmentation-based sequencing.

Representative examples of the quantitation procedure applied to phospho-tyrosine (g-h) and phospho-serine (i-j) peptides found in two biological replicate experiments are shown. (g, i) Chromatography elution time profiles (pre-alignment) for the indicated m/z window (m/z ± (m/z)/20,000, approximately ± 0.05 Da in these examples) are plotted for all runs. Each biological replicate had two samples, Control and Ox-PAPC treated, and each sample was run twice. The indicated ratio and t-test p-value for each phosphopeptide were calculated as described in the Methods section. An asterisk (*) indicates that the peptide was sequenced by fragmentation in that run and assigned to the peak based on SEQUEST results. The remaining peaks were identified via alignments. (h, j) Elution time versus m/z peak contour plots are shown for two representative runs at two different magnifications. In the contour plots, the conserved constellation-like pattern of adjacent peaks at different magnification levels illustrates the conserved neighboring peaks present across samples that allows the chromatography alignment approach to work. Furthermore, the rarity of peaks within the high accuracy m/z peak width windows (±0.05 Da) reduces the chance of incorrect peak identification via alignment. The red arrows indicate the peaks used for quantitation. The red boxes in the upper panels indicate the zoomed region shown in the lower panels. Note that in the contour plots, the contour (density) plotting algorithm may merge proximal isotope peaks upon zoom out, and the presence of a high intensity peak can make a lower intensity peak undetectable since the mass spectrometry data spans multiple orders of magnitude.

Supplemental Figure 1a

Mass spectrometry raw data
(multiple samples with replicates)

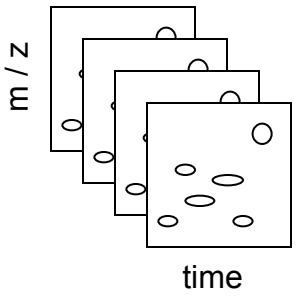

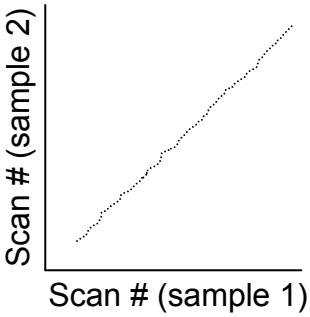

1. Chromatographic alignment using a time warping algorithm (reference 23)

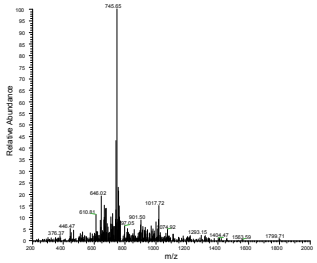

2. Peptide peak identification by MS2 sequencing

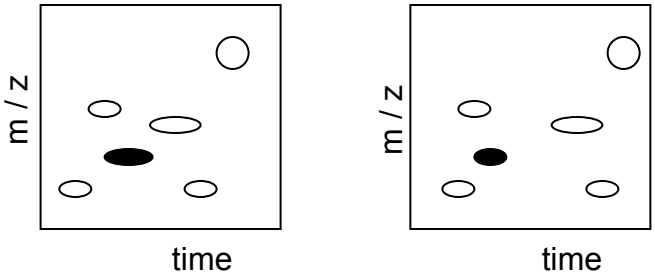

3. Peptide peak identification by alignment

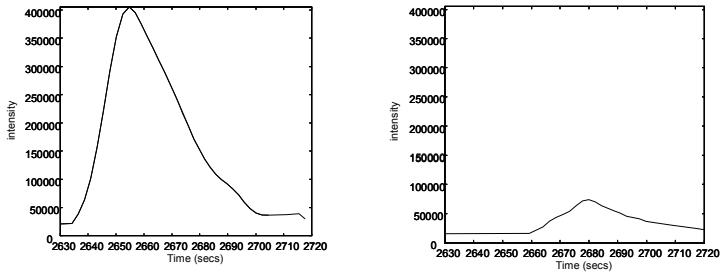

4. Quantitation of maximal peak intensity

5. Visual inspection of all peaks and manual correction of any misaligned peaks

Supplemental Figure 1b

Pre-alignment

y-axis:
vs Exp#1,Control,Run #1
vs Exp#1,Control,Run#2
vs Exp#1,Ox,Run#1
vs Exp#1,Ox,Run#2
vs Exp#2,Control,Run#1
vs Exp#2,Control,Run#2
vs Exp#2,Ox,Run#1

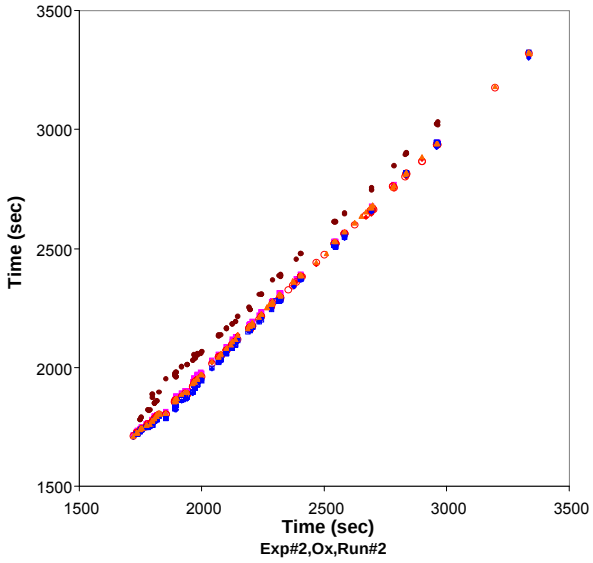

Supplemental Figure 1c

Chromatography alignment

Aligned features
Elution times of phospho-peptides sequenced in both runs

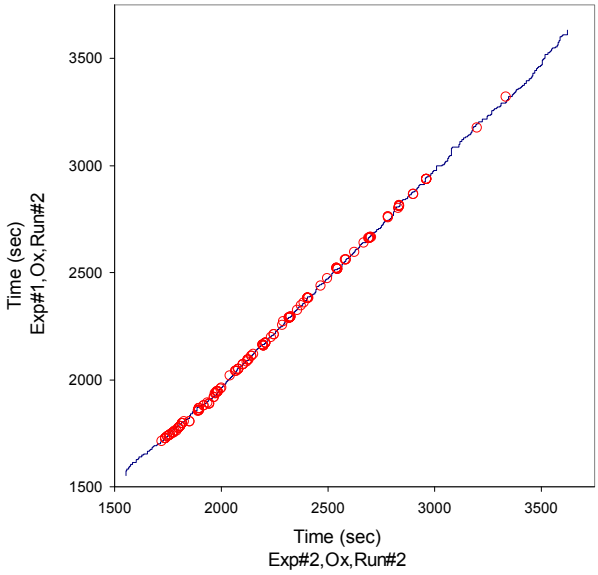

Supplemental Figure 1d

Post-alignment

y-axis:
vs Exp#1,Control,Run #1
vs Exp#1,Control,Run#2
vs Exp#1,Ox,Run#1
vs Exp#1,Ox,Run#2
vs Exp#2,Control,Run#1
vs Exp#2,Control,Run#2
vs Exp#2,Ox,Run#1

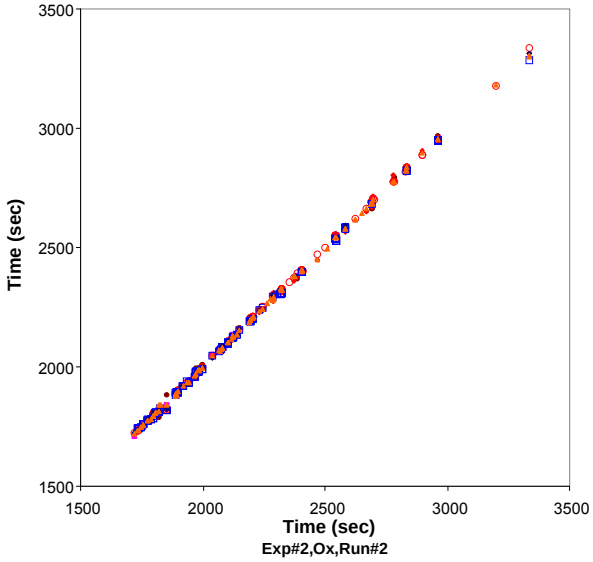

Supplemental Figure 1e

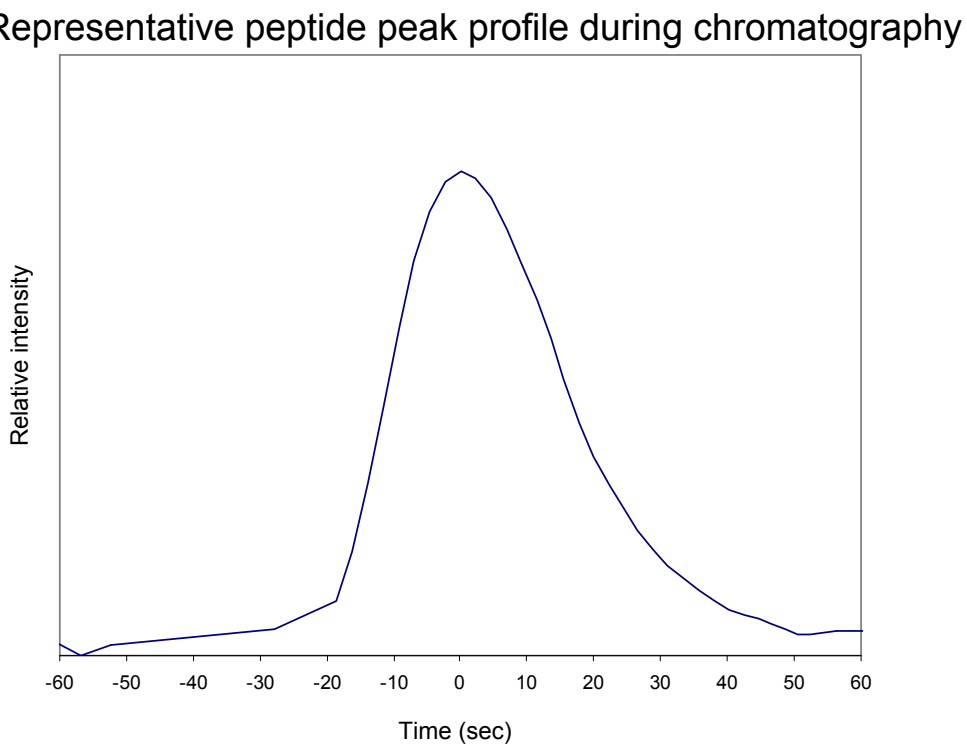

Supplemental Figure 1f

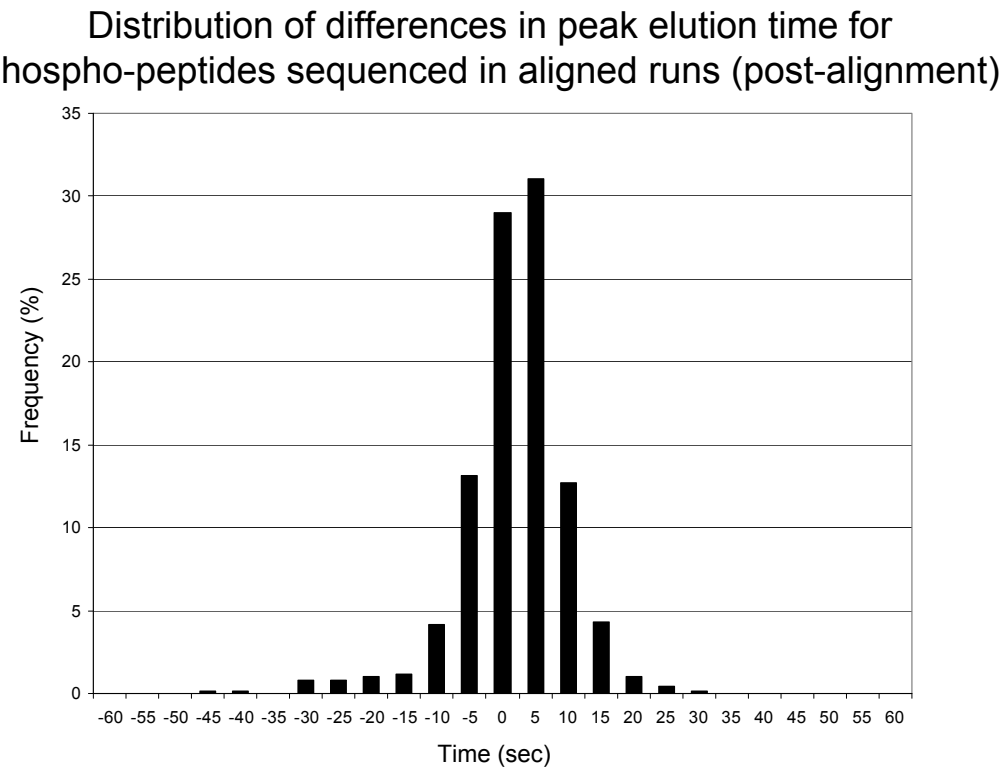

Supplemental Figure 1g

Phosphopeptide: ELFDDPSyVNVQNLDK (SHC1), m/z = 988.43
Ratio = 5.09 ; t-test = 0.014

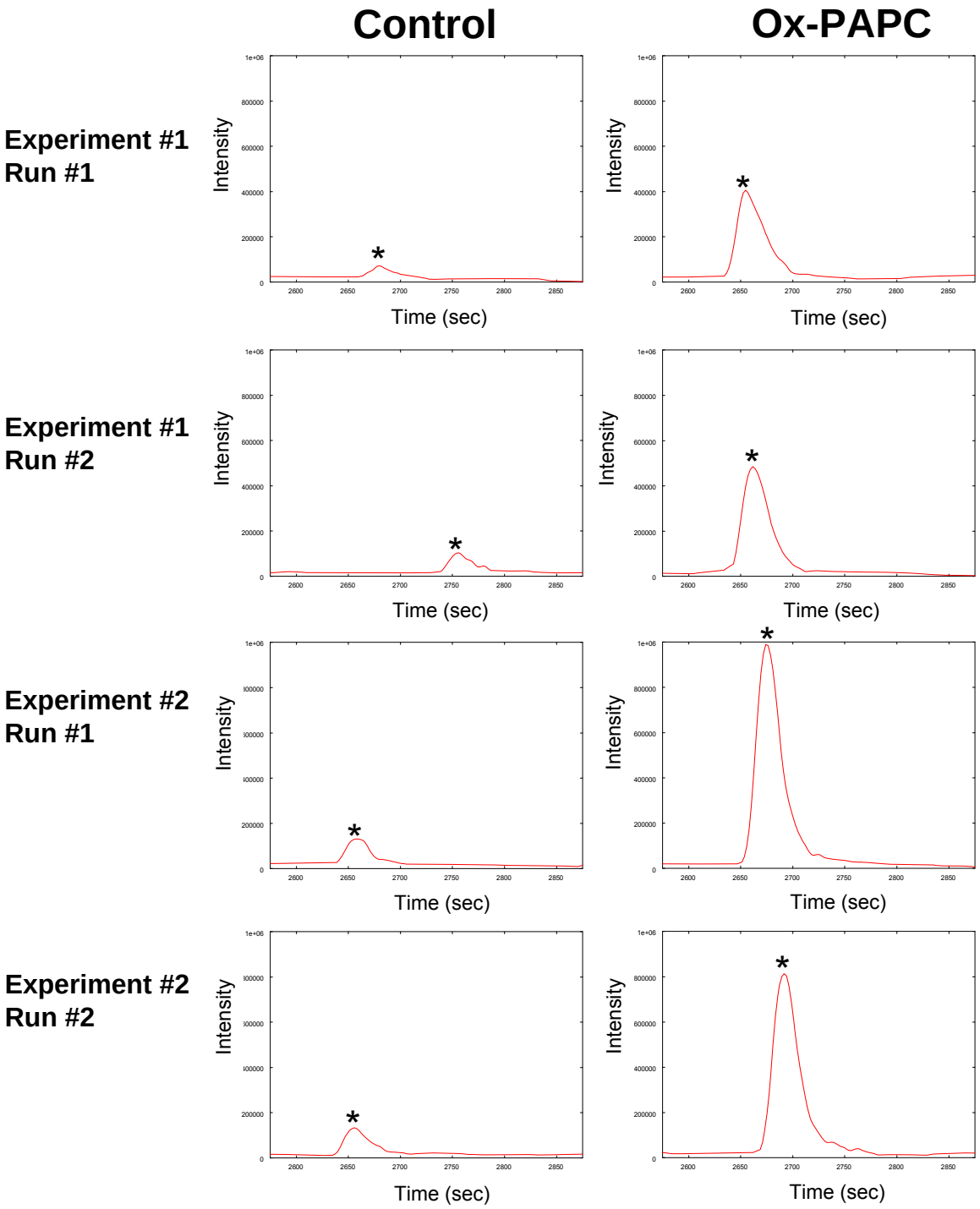

	Control		Ox-PAPC		Ratio (Ox-PAPC / Control)	t-test (p-value)
	Run #1	Run #2	Run #1	Run #2		
Experiment #1	71947	102990	405282	484610	5.09	0.014
Experiment #2	131909	133148	988857	813662	6.80	0.013

Supplemental Figure 1h

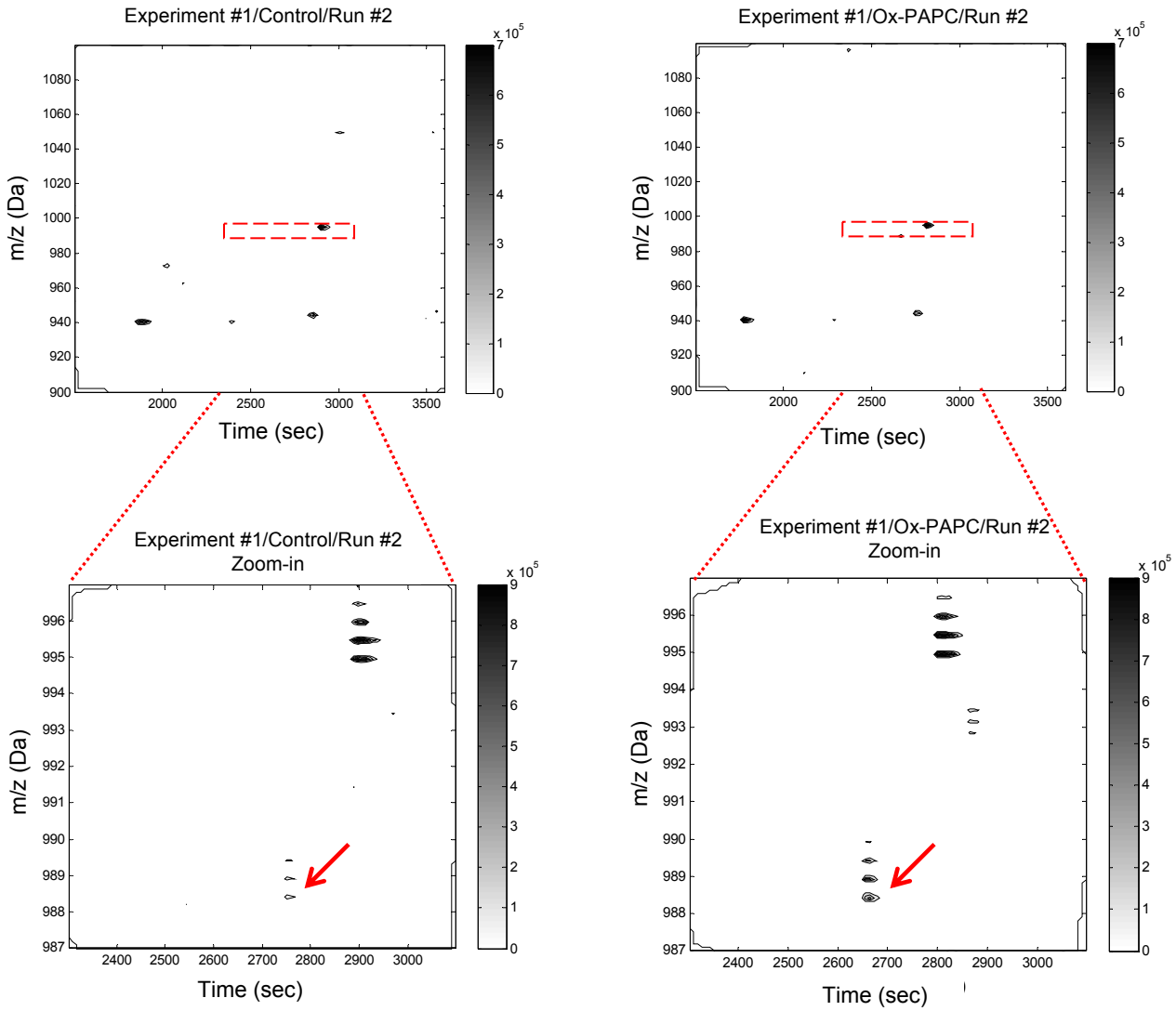

Supplemental Figure 1i

Phosphopeptide: ALQGDQTsDEEKDF (SLIRP), m/z = 831.83
Ratio ≡ 1

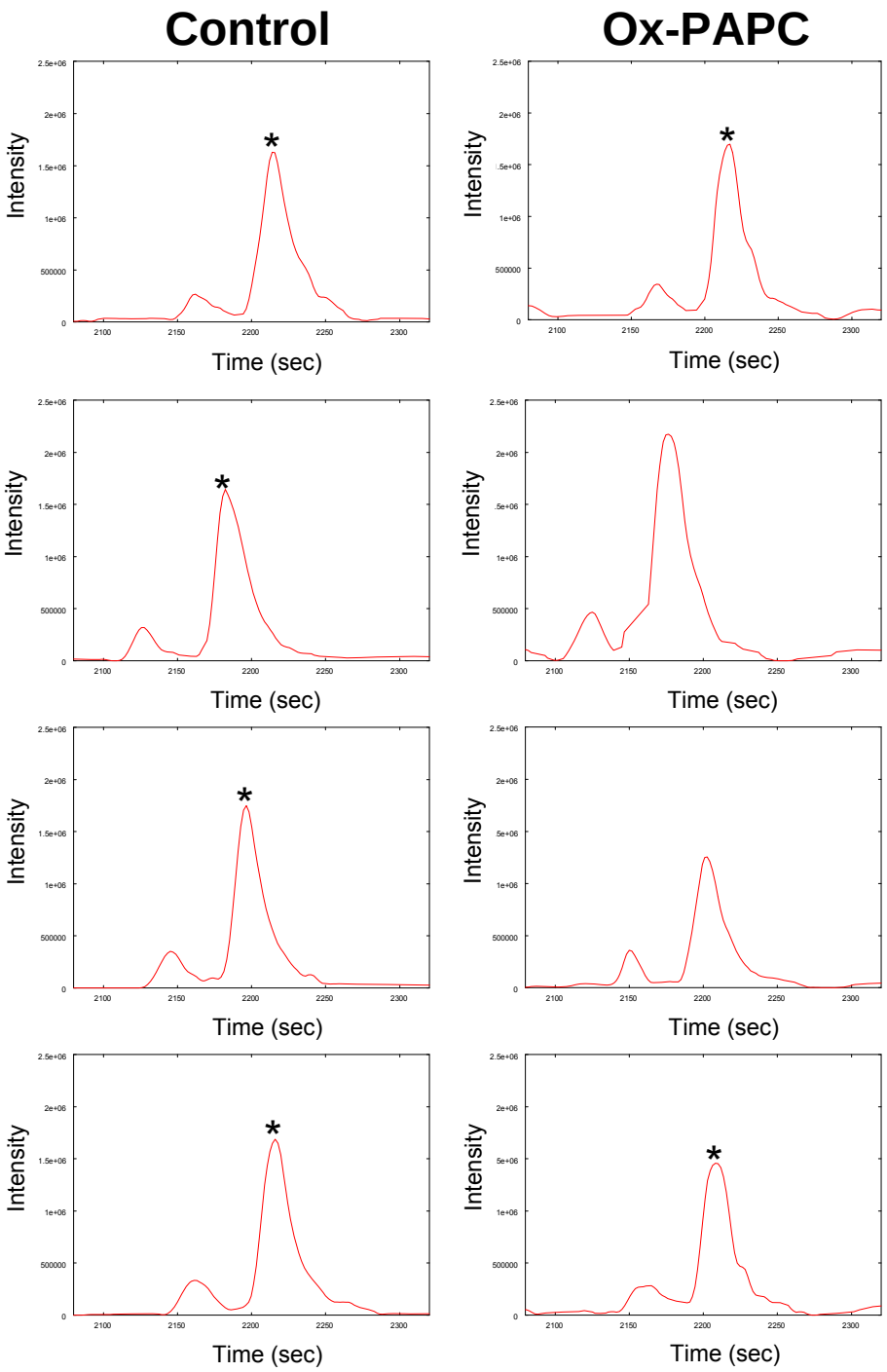

	Control		Ox-PAPC		Ratio (Ox-PAPC / Control)	t-test (p-value)
	Run #1	Run #2	Run #1	Run #2		
Experiment #1	1629600	1642720	1698197	2172779	1.18	0.334
Experiment #2	1750379	1688720	1258717	1455363	0.79	0.072

Supplemental Figure 1j

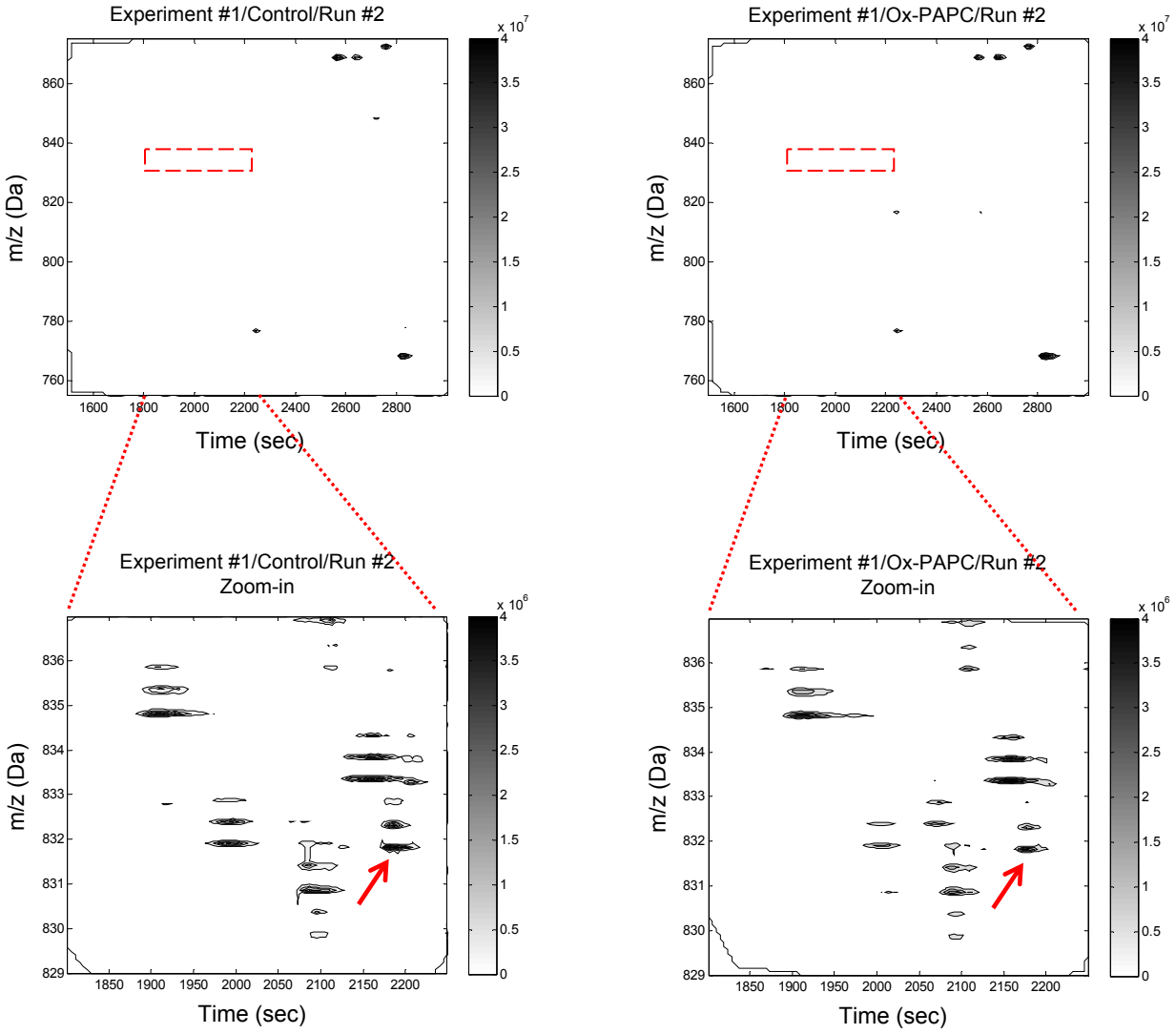

Supplemental Figure 2

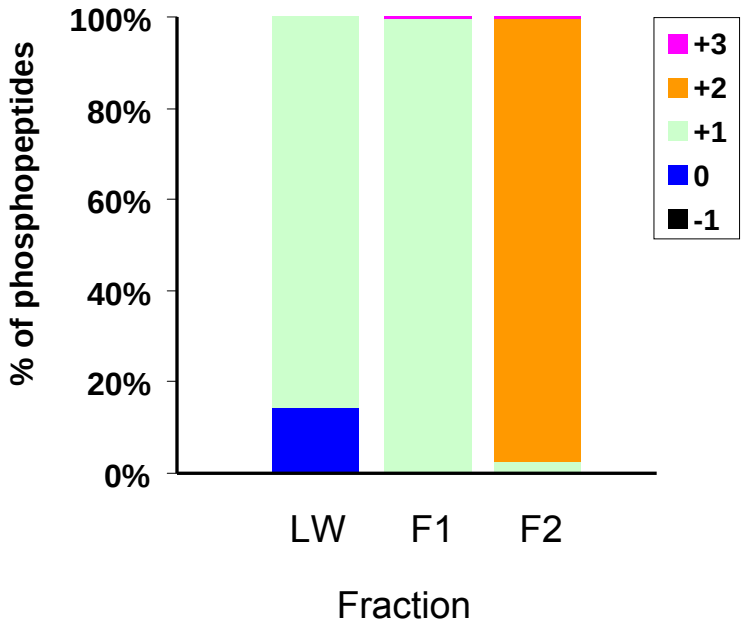

Supplemental Figure 2. Distribution of phosphopeptides in the SCX chromatography fractions based on their solution charge state at pH 2.7. Solution charge state was calculated by adding +1 for every His, Arg, Lys, and the amino terminus present in the sequence, and subtracting -1 for each phosphorylation.

Supplemental Figure 3

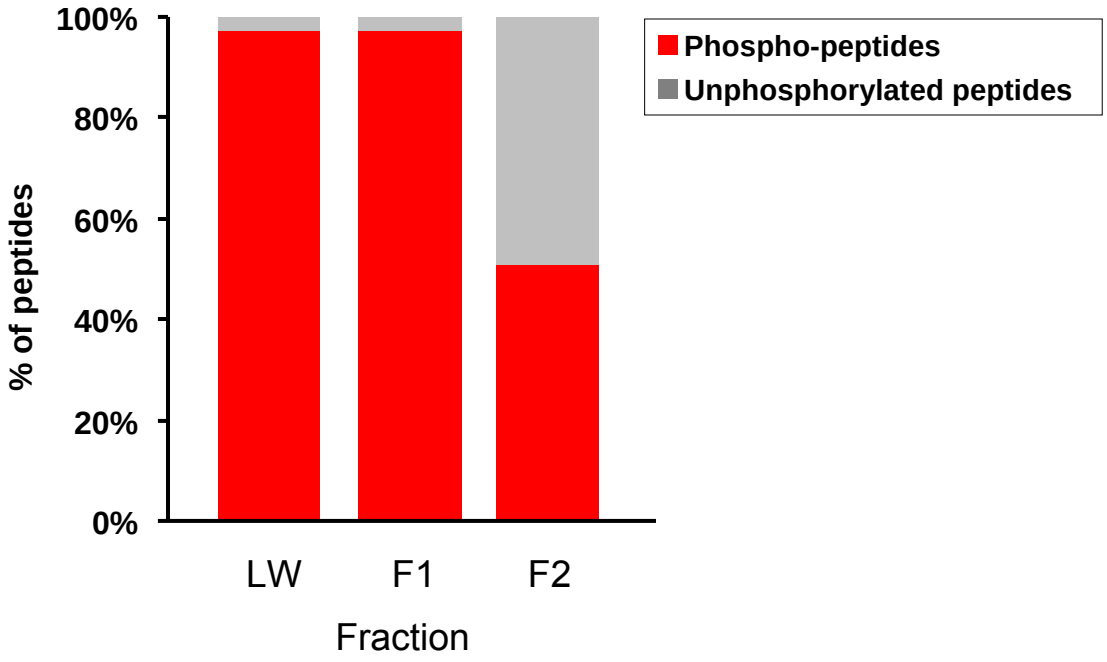

Supplemental Figure 3. Percentage of phosphopeptides present in each fraction after separation by SCX chromatography and enrichment of phosphopeptides using TiO2 metal affinity.

Supplemental Figure 4

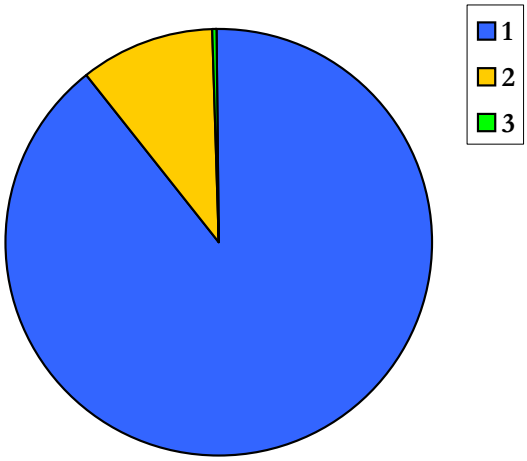

Supplemental Figure 4. Distribution of phosphopeptides based on the number of phosphate groups found after enrichment of phosphopeptides by SCX-TiO_2.

Supplemental Figure 5. Determination of significant phosphorylation changes induced by Ox-PAPC based on ratio and t-test p-value comparisons between different and like samples. Plots show the ratio (log_2) versus t-test p-value ($-log_{10}$) between control and Ox-PAPC-treated aortic endothelial cells for all phosphorylation events identified (red squares and blue triangles), estimated false positive distributions based on like biological replicates (black diamonds), and the corresponding thresholds for determination of significant induction or repression. Results are shown for peptides enriched by phospho-tyrosine antibody (pY-IP; a,b) and by SCX-TiO_2 (c,d). Results are separated in two groups depending on if the phosphopeptides were quantified twice (in which case the worst ratio and t-test p-value are plotted) (a,c) or once (b,d). A set of estimated false positive (FP) results were calculated using like biological replicates (control vs. control and Ox-PAPC vs. Ox-PAPC; black diamonds) to determine if Ox-PAPC induced phosphorylation events (red squares) or dephosphorylation (blue triangles) were statistically significant. Ratio and t-test p-value thresholds yielding a false positive rate of less than 1% are indicated by dotted lines and phosphopeptides beyond these thresholds are listed as induced by Ox-PAPC in Tables 1 and 2 and Supplementary Tables 1 and 2.

Supplemental Figure 5